G551D and G1349D, Two CF-associated Mutations in the Signature Sequences of CFTR, Exhibit Distinct Gating Defects

Silvia G. Bompadre,[1,2] Yoshiro Sohma,[2,3] Min Li,[1,2] and Tzyh-Chang Hwang[1,2]

[1]Department of Medical Pharmacology and Physiology, [2]Dalton Cardiovascular Research Center, University of Missouri-Columbia, Columbia, MO 65211
[3]Department of Physiology, Osaka Medical College, Takatsuki, Osaka 569-8686, Japan

Mutations in the gene encoding cystic fibrosis transmembrane conductance regulator (CFTR) result in cystic fibrosis (CF). CFTR is a chloride channel that is regulated by phosphorylation and gated by ATP binding and hydrolysis at its nucleotide binding domains (NBDs). G551D-CFTR, the third most common CF-associated mutation, has been characterized as having a lower open probability (Po) than wild-type (WT) channels. Patients carrying the G551D mutation present a severe clinical phenotype. On the other hand, G1349D, also a mutant with gating dysfunction, is associated with a milder clinical phenotype. Residues G551 and G1349 are located at equivalent positions in the highly conserved signature sequence of each NBD. The physiological importance of these residues lies in the fact that the signature sequence of one NBD and the Walker A and B motifs from the other NBD form the ATP-binding pocket (ABP1 and ABP2, named after the location of the Walker A motif) once the two NBDs dimerize. Our studies show distinct gating characteristics for these mutants. The G551D mutation completely eliminates the ability of ATP to increase the channel activity, and the observed activity is ∼100-fold smaller than WT-CFTR. G551D-CFTR does not respond to ADP, AMP-PNP, or changes in [Mg^{2+}]. The low activity of G551D-CFTR likely represents the rare ATP-independent gating events seen with WT channels long after the removal of ATP. G1349D-CFTR maintains ATP dependence, albeit with a Po ∼10-fold lower than WT. Interestingly, compared to WT results, the ATP dose–response relationship of G1349D-CFTR is less steep and shows a higher apparent affinity for ATP. G1349D data could be well described by a gating model that predicts that binding of ATP at ABP1 hinders channel opening. Thus, our data provide a quantitative explanation at the single-channel level for different phenotypes presented by patients carrying these two mutations. In addition, these results support the idea that CFTR's two ABPs play distinct functional roles in gating.

INTRODUCTION

CFTR, a member of the ATP-binding cassette (ABC) transporter family, is a chloride channel that is gated by ATP binding and hydrolysis. By analogy to other ABC transporters, it is proposed that an ATP-driven dimerization of CFTR's two nucleotide binding domains (NBD1 and NBD2) leads to the opening of the channel, and hydrolysis at NBD2 leads to dimer dissociation and, consequently, closing of the channel (for reviews see Gadsby et al., 2006; Zhou and Hwang, 2007). Once the two NBDs dimerize, each ATP-binding pocket (ABP) is composed of the Walker A and B motifs of one NBD and the signature sequence of the partner NBD (Fig. 1). We therefore define, here, ABP1 as the binding site that consists of the Walker A and B motifs from the N-terminal NBD (i.e., NBD1) and the signature sequence from the C-terminal NBD (i.e., NBD2). An equivalent definition is made for ABP2.

Mutations in the CFTR gene cause the genetic disease cystic fibrosis (Riordan et al., 1989), the most common lethal autosomal recessive disorder in Caucasian populations (Riordan et al., 1989; Welsh and Smith, 1993;

Tsui and Durie, 1997). CF is manifested by a defective chloride transport across the epithelial cells in various tissues such as respiratory, gastrointestinal, hepatobiliary, and reproductive tracts (Quinton, 1990). More than 1,400 mutations have been identified as disease associated in the cystic fibrosis mutation database (www.genet.sickkids.on.ca/). These mutations can be divided into four classes based on the mechanisms that disrupt CFTR function (Welsh and Smith, 1993): defective protein production (I); defective protein processing (II); defective activation and regulation (III), including G551D and G1349D; and defective conductance (IV).

G551D is the third overall most common CF mutation with a worldwide frequency of ∼3% (www.genet.sickkids.on.ca/cftr). This mutation is associated with a severe phenotype characterized by pulmonary dysfunction and pancreatic insufficiency (Cutting et al., 1990; Kerem et al., 1990). The result of this glycine-to-aspartate mutation at position 551 is a significantly decreased

Correspondence to Tzyh-Chang Hwang: hwangt@health.missouri.edu

chloride current due to a drastic reduction of the channel activity (Drumm et al., 1991). The importance of the G551 residue also lies in the fact that it is located in the signature sequence of CFTR's NBD1 (Fig. 1). Interestingly, the corresponding residue, G1349, in the signature sequence of NBD2, has also been identified as disease associated when it is mutated to aspartate (Beaudet et al., 1991). However, the G1349D mutation is associated with a milder clinical phenotype (Brancolini et al., 1995, Salvatore et al., 2002).

Although G551D-CFTR and G1349D-CFTR have been used in pharmacological studies for years (e.g., Illek et al., 1999; Galietta et al., 2001; Moran et al., 2005; Pedemonte et al., 2005), little is known about the mechanism responsible for their dysfunction due to limited functional studies of these two mutants at a single-channel level (e.g., Cai et al., 2006). It is also puzzling why analogous mutations at two equivalent positions would cause different phenotypes if the two ABPs were equally important in opening CFTR channels as proposed previously (Vergani et al., 2003; c.f. Zhou et al., 2006). Gregory et al. (1991) reported that these two mutant proteins have normal biosynthesis, trafficking, and processing. Using a fluorescence-based assay they observed that G551D-CFTR channels lack functional activity, even though the channels can be normally phosphorylated in the R domain (Chang et al., 1993). Logan et al. (1994) reported that as a consequence of the G551D, or G1349D mutation, nucleotide binding to isolated recombinant NBD1 and NBD2 is decreased. The significance of this early biochemical study is unclear in light of the latest finding that CFTR's two NBDs likely dimerize with ATP molecules sandwiched at the dimer interface as seen in other ABC transporters (Vergani et al., 2005). Wilkinson et al. (1996) measured the rates of activation and deactivation of macroscopic CFTR currents in *Xenopus* oocytes and found that the apparent on rate of channel activation by cAMP for G551D-CFTR or G1349D-CFTR was drastically reduced. A possible explanation for this reduction is an increase of the closed time of the channel, as demonstrated by Cai et al. (2006). However, the low Po of these two mutants makes it very difficult to accurately quantify single channel kinetics.

We have studied the response of G551D-CFTR and G1349D-CFTR to ATP, ADP, and AMP-PNP in excised inside-out membrane patches. Although both mutants show lower Po than WT-CFTR, as shown previously (Li et al., 1996; Cai et al., 2006), they exhibit very different behaviors. The G551D mutation completely abolishes the response of the channel to ATP and ADP, whereas the G1349D mutation remains responsive to ATP and the ATP-induced activity can be inhibited by ADP. These results are consistent with the idea that ATP binding to the ABP2 site (formed by the signature sequence of NBD1 and the Walker A and B motifs of NBD2) is
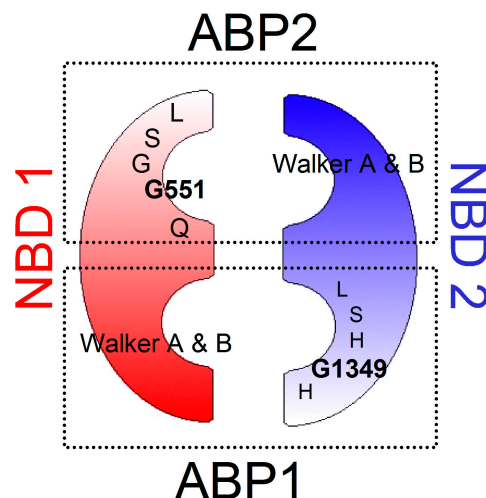

Figure 1. Cartoon depicting the location of G551 and G1349 in CFTR's two ATP-binding pockets. The G551 residue is located in the signature sequence of NBD1 while the G1349 is located in the signature sequence of NBD2. CFTR has two ATP-binding pockets (ABPs) composed by the Walker A and B motifs of one NBD and the signature sequence of the partner NBD. The ATP-binding pockets are named after the position of the Walker A motif (i.e., ABP1 is composed of the Walker A and B motifs of NBD1 and the signature sequence of NBD2). Thus the G551D mutation is located in ABP2 and the G1349D mutation is located in ABP1.

critical to catalyze ATP-dependent channel opening (Vergani et al., 2003; Berger et al., 2005; Bompadre et al., 2005b; Zhou et al., 2006). Interestingly, compared with WT data, the ATP dose–response relationship for G1349D-CFTR is less steep and shows an increase of the apparent affinity for ATP. These features of the ATP dose response for G1349D-CFTR could be reproduced by assuming that ATP binding to ABP1, where the mutation is located, hinders channel opening. The fundamental mechanism responsible for the different behavior of these two mutant channels and the potential clinical implications of our results will be discussed.

MATERIALS AND METHODS

Site-directed Mutagenesis
The construction of the expression vector pcDNA 3.1 Zeo(+) (Invitrogen) containing WT CFTR cDNA has been described previously (Powe et al., 2002). Point mutations (G551D and G1349D) were introduced into WT-CFTR by QuikChange XL method (Stratagene). The entire CFTR cDNA was sequenced (DNA core, University of Missouri-Columbia) to confirm the mutation. This strategy has been routinely used in our laboratory to obtain mutant CFTR constructs.

Cell Culture and Transient Expression
CHO cells were grown at 37°C and 5% CO$_2$ in Dulbecco's modified Eagle's medium supplemented with 10% FBS. To transiently express CFTR, CHO cells were grown in 35-mm tissue culture dishes 1 d before transfection. The DNA construct, encoding WT or mutant CFTR, was cotransfected with pEGFP-C3 (CLONTECH Laboratories Inc.) encoding GFP using SuperFect transfection
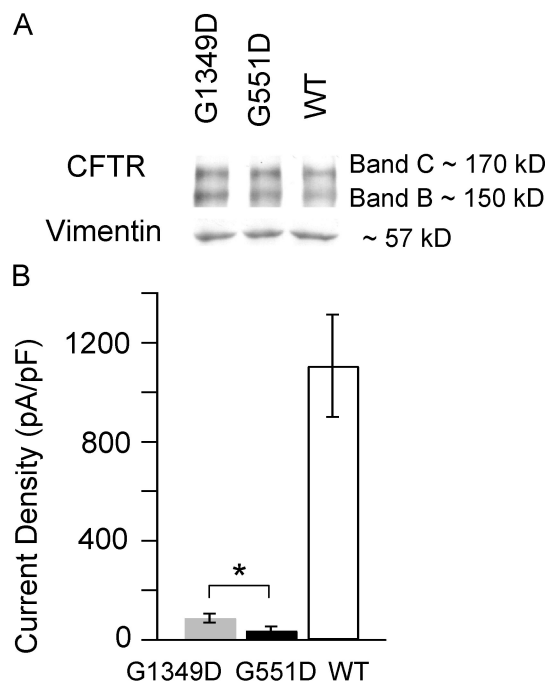
Figure 2. G551D-CFTR and G1349D-CFTR expression in CHO cells. (A) Western blot analysis for WT-, G551D-, and G1349D-CFTR. Mature fully glycosylated CFTR and core-glycosylated CFTR are labeled as Band C and Band B, respectively. The same blot was probed with an antibody against the cytoskeletal protein vimentin as a control for protein loading. Similar results were obtained in three separate preparations. (B) Mean current densities obtained from whole-cell experiments for G551D ($n = 30$), G1349D ($n = 29$), and WT ($n = 20$). Columns and error bars indicate means ± SEM, * indicates P < 0.01 between G551D and G1349D.

reagent (QIAGEN) according to the manufacturer's protocols. The transfected cells were used for electrophysiological studies 2–6 d after transfection.

Western Blot Analysis

48 h after transfection, cells from confluent 35-mm dishes were washed with PBS and lysed in 1× Laemmli sample buffer (Bio-Rad Laboratories Inc.). DNA was sheared by brief sonication. Whole cell lysates were separated on 7.5% Tris-HCl SDS-PAGE gels (Bio-Rad Laboratories Inc.) and transferred onto a nitrocellulose membrane. The membrane was blocked with 5% milk in TBST buffer (20 mM Tris, 137 mM NaCl, 0.05% Tween) at room temperature for 1 h and then probed with primary antibody against CFTR (clone M3A7, Chemicon) in PBS at 4°C overnight. M3A7 is a mouse monoclonal antibody that recognizes an epitope at the C-terminal end, in the region of residues 1370 to 1380. The membrane was washed with TBST three times and then incubated with the horseradish peroxidase–conjugated secondary antibody (donkey anti-mouse IgG; Jackson ImmunoResearch Laboratories) for 2 h at room temperature. The membrane was developed with chemiluminescence reagent (Pierce Chemical Co.) for 5 min and exposed to film (Fuji Photo Film Co.). The blot was stripped and reprobed with an anti-vimentin antibody (C-20, Santa Cruz Biotechnology Inc.) as an internal control of protein loading.

Electrophysiological Recordings and Data Analysis

All data were recorded at room temperature using an EPC9 amplifier (HEKA). For whole-cell recordings, the membrane potential was held at 0 mV. Current traces were filtered at 1 kHz

with a built-in four-pole Bessel filter, and then digitized to the computer at a sampling rate of 2 kHz. Ramp voltages to −100 mV (in 400 ms) and to +100 mV (in 400 ms) were generated with Pulse software (HEKA). The net current was calculated as the current between 0 and +100 mV minus the basal current at the same voltages (leak current) using Igor software (Wavemetrics). The membrane capacitance was obtained from the EPC9 amplifier after the compensation of the capacitance current. The mean current density was calculated as the ratio between the net mean current and the membrane capacitance. The bath solution contained (in mM) 145 NaCl, 5 KCl, 2 $MgCl_2$, 1 $CaCl_2$, 5 glucose, and 5 HEPES (pH 7.4 with NaOH). 20 mM sucrose is added to the bath solution to prevent activation of swelling-induced currents. The pipette solution contained (in mM) 10 EGTA, 10 HEPES, 20 TEACl, 10 MgATP, 2 $MgCl_2$, 101 CsCl, and 5.8 glucose.

For inside-out recordings, the membrane potential was held at −50 mV for all experiments. Data were filtered at 100 Hz with an eight-pole Bessel filter (Warner Instrument) and digitized at a sampling rate of 500 Hz. Downward deflections in the current trace indicate channel opening. The pipette solution contained (in mM) 140 NMDG-Cl, 2 $MgCl_2$, 5 $CaCl_2$, and HEPES (pH 7.4 with NMDG). The standard perfusion solution for inside-out patches contained (in mM) 150 NMDG-Cl, 10 EGTA, 10 HEPES, 8 TRIS, and 2 $MgCl_2$ (pH 7.4 with NMDG). For experiments with magnesium-free solutions, we used a formula based on Dousmanis et al. (2002). EGTA in the perfusion solution was substituted with 2 mM CDTA to buffer magnesium.

The steady-state mean current and single channel amplitudes were calculated with Igor. Open times were calculated using a program developed by Csanady (2000) from recordings with up to four channel open steps (for details see Bompadre et al., 2005a). In brief, current traces were baseline corrected, idealized, and fitted to a three-state model C↔O↔B, where O and C are open and closed states, respectively. B is a blocked state induced by an intrinsic blocker (Zhou et al., 2001). To determine the true ATP-dependent parameters, the ATP-independent brief closures (flickers) observed within a burst had to be removed. The rate constants r_{CO}, r_{OC}, r_{OB}, and r_{BO} are extracted by a simultaneous fit to the dwell-time histograms of all conductance levels. Mean burst durations were calculated as $\tau_b = (1/r_{OC})(1 + r_{OB}/r_{BO})$. Then, the burst time ($\tau_b$) corresponds to the ATP-dependent open time of the channel. For kinetic modeling, we employed the Q-matrix method (Colquhoun and Hawkes, 1995) to calculate the steady-state solution for the open probability for Schemes A and B (Figs. 10 and 11).

Statistics

Results are expressed as means ± SEM for n cells. To compare data, Student t tests were performed using SigmaPlot (SPSS Science, version 8.0.2); P < 0.01 was considered statistically significant.

Reagents

Mg-ATP and ADP were purchased from Sigma-Aldrich. PKA was purchased from Promega. AMP-PNP was purchased from Roche and stored as 250 mM stock in H_2O at −20°C.

RESULTS

Expression of G551D-CFTR and G1349D-CFTR

It has been previously reported that neither G551D-CFTR nor G1349D-CFTR exhibit trafficking defects in COS cells (Gregory et al., 1991). To ensure that abnormal trafficking was also absent when these mutants are expressed in CHO cells, we performed a Western blot analysis.
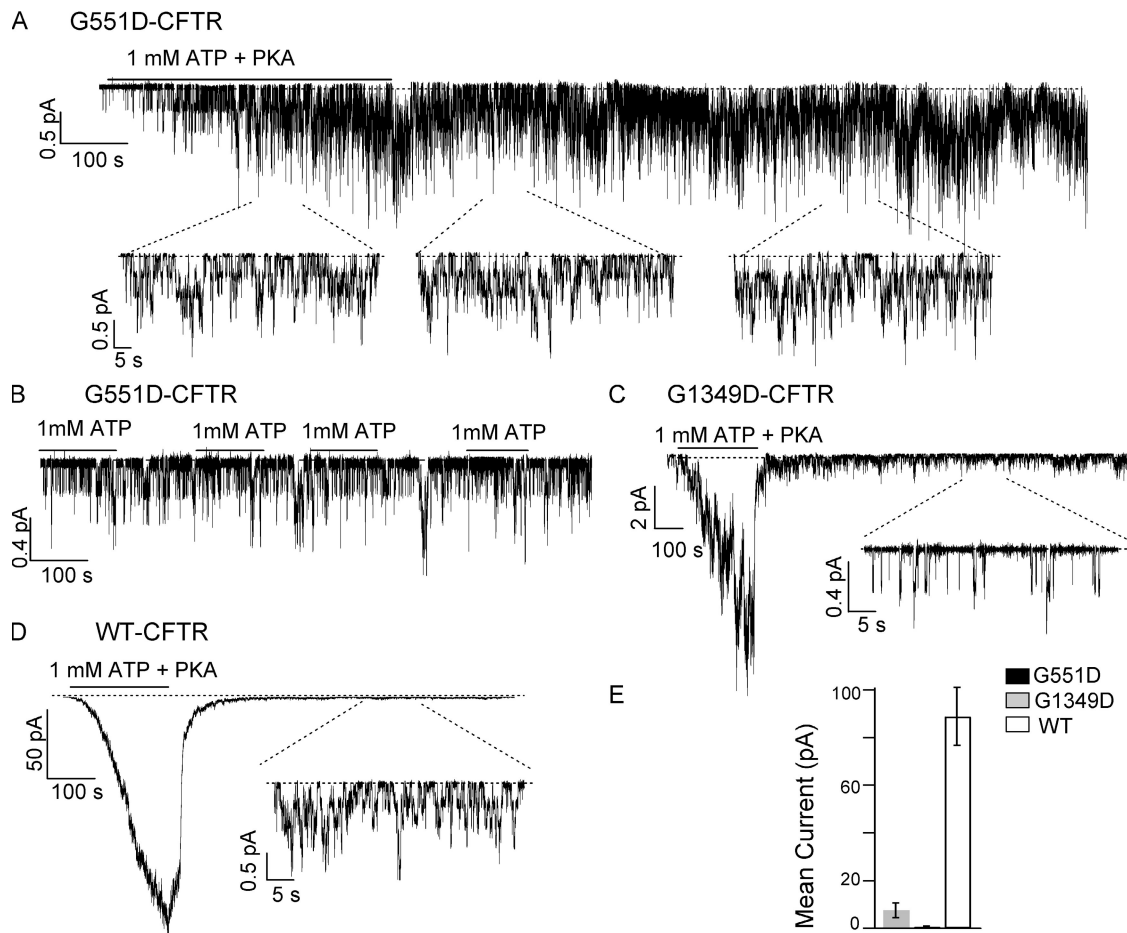
Figure 3. Gating of G551D-CFTR and G1349D-CFTR in excised inside-out membrane patches. (A) A recording of G551D-CFTR channel currents in an excised inside-out membrane patch. Note that after washout of ATP and PKA, the channels remained active for over 20 min. Expanded current traces show the G551D-CFTR channel activity in the presence of ATP + PKA and during washout. (B) Repeated addition and removal of ATP in the same patch did not result in significant changes of the channel activity of G551D-CFTR. (C) A recording of G1349D-CFTR channel currents in an excised inside-out membrane patch. The channels were activated with 1 mM ATP + 25 U/ml PKA. Upon removal of ATP and PKA, the current decays very rapidly. A small amount of current remains minutes after washout of ATP. (D) A recording of WT-CFTR channel currents in an excised inside-out membrane patch. (E) Comparisons of mean macroscopic current amplitude for G551D- ($n = 16$), G1349D- ($n = 18$), and WT-CFTR ($n = 13$). Data are presented as means ± SEM.

Fig. 2 A shows that the relative amount of fully glycosylated proteins (band C) is not different between these two mutants and WT-CFTR, confirming that these mutant proteins can fold and traffic normally to the plasma membrane in CHO cells.

It is known that the cAMP-activated currents for these two CFTR mutants are extremely small (Drumm et al., 1991; Anderson and Welsh, 1992). If we assume that plasma membrane expression of WT-CFTR and these two mutants is about the same, we can then use the whole-cell cAMP-dependent current as a marker to quantitatively estimate the gating defects caused by these two mutations. We transfected CHO cells with WT-CFTR, G551D-CFTR, and G1349-CFTR, in parallel, using the same amount of DNA. Whole-cell patch-clamp experiments were also performed in parallel to minimize variations. Once the whole-cell configuration was obtained, chloride currents were elicited with 10 μM

forskolin. The mean current density was calculated as the ratio between the net mean current at +100 mV and the membrane capacitance. Fig. 2 B shows that the current densities of G551D ($n = 30$) and G1349D ($n = 29$) mutants are lower than that of WT-CFTR ($n = 20$). However, the current density of G1349D-CFTR is significantly larger than that of G551D-CFTR (P < 0.01), suggesting that the Po of G1349D-CFTR is higher than that of G551D-CFTR.

ATP-dependent Gating of G551D-CFTR and G1349D-CFTR
To investigate the mechanism responsible for the different gating behavior of G551D and G1349D mutants, we studied both mutants in excised inside-out membrane patches. First we examined the ATP-dependent gating properties of these mutants. After the membrane patch was excised into the inside-out configuration, channels were activated by 1 mM ATP + 25 U/ml PKA.
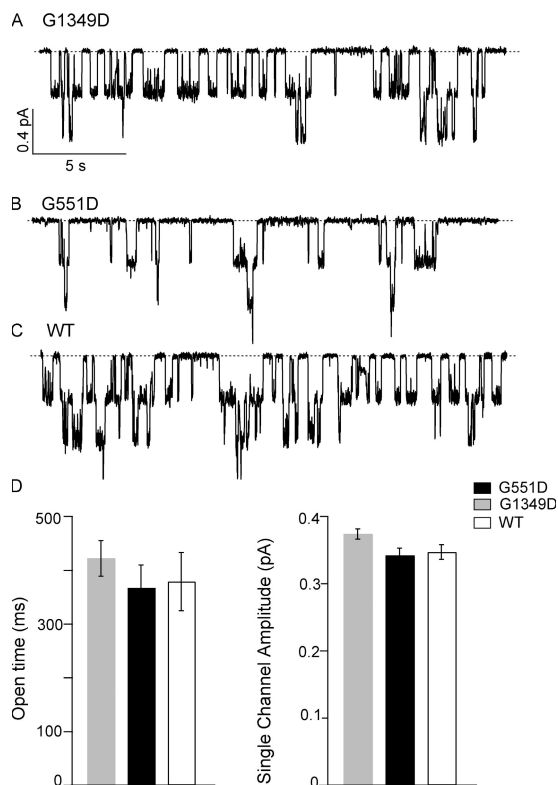
Figure 4. Comparison of the mean open times of G551D-, G1349D-, and WT-CFTR. (A) Expanded single-channel current traces in the presence of 1 mM ATP for G551D-, G1349D-, and WT-CFTR. (B) Comparisons of the mean open times and single channel amplitudes ($n = 6$–14 for each data point). Data are presented as means ± SEM.

Figure 5. Effect of $[Mg^{2+}]$ in the closing rate of WT and G551D-CFTR. Currents were activated by 1 mM ATP + PKA in a Mg^{2+}-containing solution. (A) Withdrawal of ATP + PKA and Mg^{2+} ions results in channels closing more slowly for WT-CFTR. Note that some channels remain open for tens of seconds. (B) G551D-CFTR channel openings remain unaltered when ATP, PKA, and Mg^{2+} are removed from the perfusion solution ($n = 6$).

In the case of G551D-CFTR, the elicited currents were usually small compared with the macroscopic current seen with WT-CFTR (Fig. 3, compare A and D). Surprisingly, when ATP and PKA were removed, the G551D-CFTR current remained unchanged for tens of minutes ($n = 46$). Fig. 3 A shows a 25-min continuous recording of G551D-CFTR. We are confident that the observed current arises from G551D-CFTR channels because no activity was observed in nontransfected cells and the observed currents were PKA dependent. The single-channel amplitude of G551D-CFTR is similar to that of WT channels (see below), and furthermore, glibenclamide, a CFTR blocker (Zhou et al., 2002), blocks G551D-CFTR currents to the same extent as it does to WT-CFTR (unpublished data). Repeated addition and removal of ATP in the same patch did not result in significant changes of the channel activity (Fig. 3 B), suggesting that G551D-CFTR channel activity is ATP independent. A similar observation was reported recently by Wang et al. (2007). When the same experiment was performed with G1349D-CFTR, we observed generally larger currents than that of G551D-CFTR (e.g., Fig. 3 C). In addition, unlike G551D-CFTR, G1349D-CFTR channel current decreases immediately upon ATP washout, a
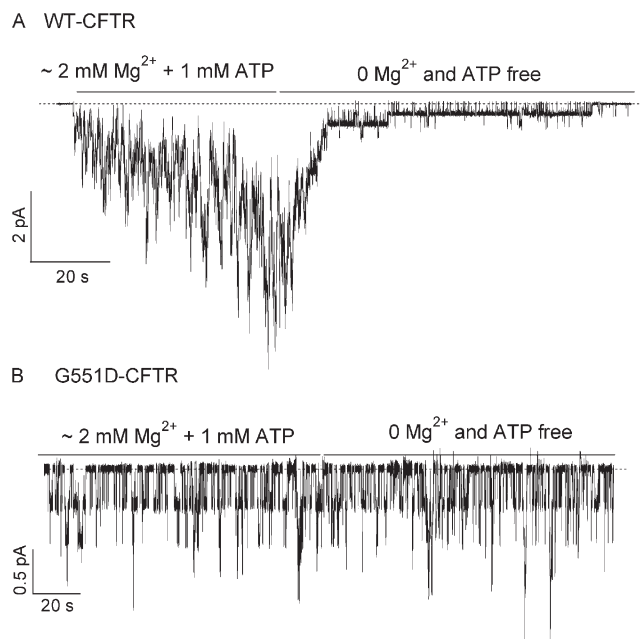
property shared with the WT channels (Fig. 3 D). Note that for both WT- and G1349D-CFTR a small but significant fraction of the current remained for minutes after nucleotide removal.

Fig. 3 E summarizes our results obtained from these experiments. The steady-state mean current amplitude (a product of the number of functional channels, Po and single-channel amplitude) shows a similar pattern as that of whole-cell recordings (i.e., WT > G1349D > G551D). It should be noted that it is very difficult to calculate accurately the Po and closed time of the channel using traditional methods due to the low open probabilities of these mutants (thus the number of functional channels cannot be ascertained). Since the single-channel amplitude is not altered by the mutations (see Fig. 4 D), we can compare the Po if we assume that the number of functional channels is roughly the same. We estimated the Po of the mutants by scaling the value of the WT Po using the mean current amplitudes shown in Fig. 3 E. This method, although not entirely precise, will give us some rough estimation of the Po values for the mutants. Since the Po for WT channels in the presence of 1 mM ATP is 0.45 ± 0.04 (see Fig. 9 D), the estimated Po are $\cong 0.0037$ for G551D (120 times smaller than the WT Po), and $\cong 0.045$ (10 times smaller than the WT Po) for G1349D. We then analyzed single-channel traces to obtain the mean open time for the mutants
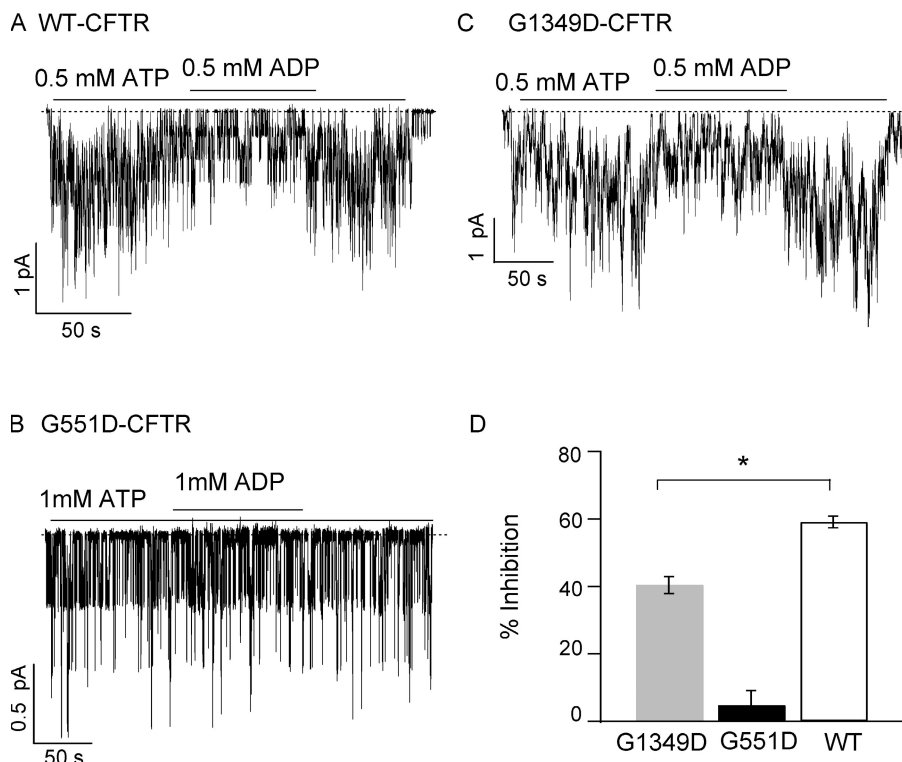
Figure 6. Effect of ADP on G551D, G1349D, and WT-CFTR. Representative current traces for WT-CFTR (A), G551D-CFTR (B), and G1349D-CFTR (C). Currents from both WT- and G1349D-CFTR are reduced by ADP, but ADP fails to inhibit G551D-CFTR channel currents. (D) Summary of percent inhibition by 500 μM ADP for G551D- ($n = 10$), G1349D- ($n = 8$), and WT-CFTR ($n = 8$). Data are presented as means ± SEM. * indicates P < 0.001 between G1349D and WT.

(see Materials and methods for details). Fig. 4 shows expanded single-channel traces for the two mutants and WT-CFTR. At 1 mM ATP, the mean open time was 367 ± 42 ms ($n = 14$) and 422 ± 33 ms ($n = 5$) for G551D- and G1349D-CFTR, respectively. Thus, the mutations do not seem to significantly alter the open time of the channels since the mean open time for WT-CFTR channels is 379 ± 54 ms ($n = 7$, from Zhou et al., 2006) at this ATP concentration. It is interesting to note that Cai et al. (2006) found that the G551D and G1349D mutations shorten the open time of the channels. Differences in experimental conditions and/or analysis methods may account for this discrepancy.

Since free $[Mg^{2+}]$ is known to affect the open time of WT-CFTR, presumably by altering the ATP hydrolysis rate (Dousmanis et al. 2002), we next examined the effect of Mg^{2+} on the closing rate of G551D- and G1349D-CFTR channels. Fig. 5 shows representative traces for WT and G551D-CFTR. Indeed, for WT-CFTR the closing rate decreases upon withdrawal of Mg^{2+} ions and ATP in the perfusion solution. That is not the case for G551D-CFTR, where the current remains unaltered when we switch from Mg^{2+}-containing solution to Mg^{2+}-free solution without ATP ($n = 6$). The mean open time for G551D-CFTR in the Mg^{2+}-free solution is 311 ± 85 ms ($n = 3$), similar to the open time observed in the Mg^{2+}-containing solution. Surprisingly, we also did not observe an increase in the open time in G1349D channels, although some ATP dependence is retained for this mutant ($n = 6$; unpublished data).

Effect of ADP and AMP-PNP on G551D-CFTR and G1349D-CFTR Channels

The results shown above indicate that G551D and G1349D, mutations at the equivalent position in the signature sequence of NBD1 and NBD2, respectively, exhibit different gating defects. To further characterize their defective functions, we examined effects of ADP and AMP-PNP on these two mutants. Previous studies have established that the presence of ATP increases the opening rate of WT-CFTR, and that ADP competes with ATP for the binding site that opens the channel (Anderson and Welsh, 1992; Winter et al., 1994; Bompadre et al., 2005a). Fig. 6 A shows a representative result for WT channels. In excised patches, after activation of the channels with 1 mM ATP + PKA, 500 μM ADP inhibits WT channel currents, elicited with 500 μM ATP, by $\sim 59 \pm 2\%$. However, ADP had little effect on G551D-CFTR currents ($n = 10$, Fig. 6 B), further confirming that G551D channel currents are ATP independent. In contrast, G1349D-CFTR channels, like WT-CFTR, can be inhibited by ADP; interestingly however, the level of inhibition was slightly but significantly less (P < 0.001), $\sim 40 \pm 3\%$ ($n = 8$, Fig. 6 C).

We then tested the nonhydrolyzable ATP analogue AMP-PNP. AMP-PNP, when applied in the presence of ATP, can lock open WT-CFTR channels for minutes (Gunderson and Kopito, 1994; Hwang et al., 1994; Mathews et al., 1998). In excised patches, after activation with 1 mM ATP + PKA, we applied 2 mM AMP-PNP + 1 mM ATP to WT (Fig. 7 A), G551D (Fig. 7 B),
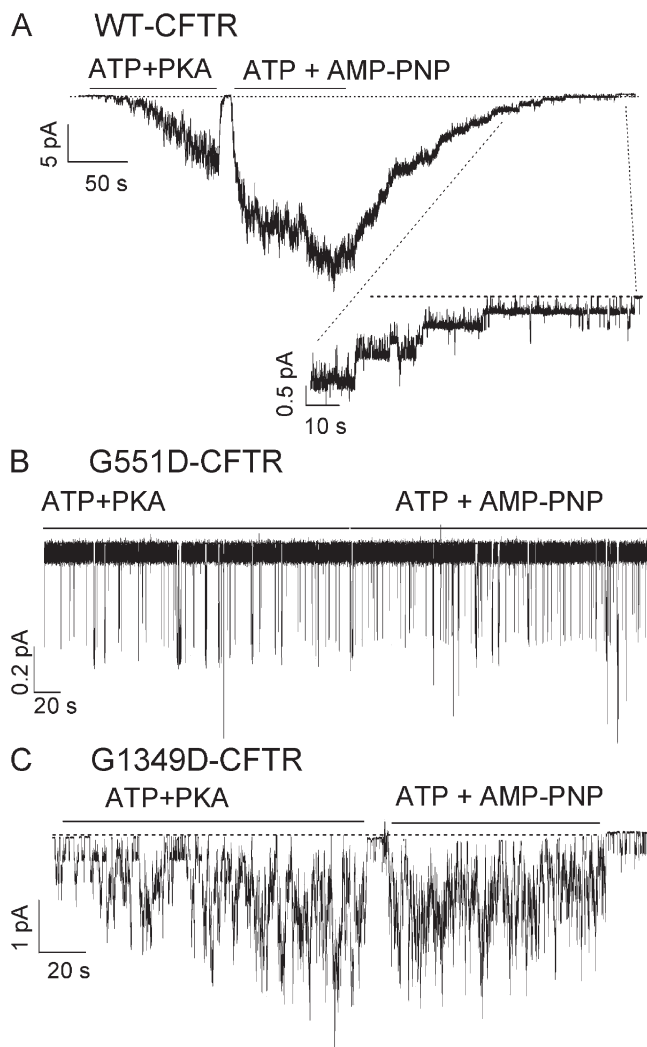
Figure 7. Effect of AMP-PNP on G551D, G1349D, and WT-CFTR. Representative current traces for WT-CFTR (A), G551D-CFTR (B), and G1349D-CFTR (C). WT-CFTR channels were locked open by 2 mM AMP-PNP + 1 mM ATP. Neither G551D- nor G1349D-CFTR responds to AMP-PNP ($n = 4$ each).

and G1349D channels (Fig. 7 C). Note that in the case of WT channels, the current was macroscopic, and single-channel closing events were observed only after a long washout. AMP-PNP locked open the WT channels. The locked open time can be obtained from the relaxation time constant upon washout of ATP and AMP-PNP. The calculated locked open time of WT- CFTR channels is ~73.5 s (from Zhou et al., 2005), which is much longer than the open time of the channels in the presence of 1 mM ATP alone (379 ± 54 ms). In contrast, AMP-PNP failed to increase either the G551D- or G1349D-CFTR currents (Fig. 7, B and C). Upon removal of the nucleotides, most of the G1349D-CFTR channel currents decreased rapidly (Fig. 7 C). We did not observe slow closures of the channels as seen with WT-CFTR.

[ATP] Dependence of G551D- and G1349D-CFTR

Our data suggest that the G551D mutation abolished nucleotide-dependent gating. It remains possible that this mutation lowers ATP binding affinity as other mutations in ABP2 (e.g., Y1219G in Zhou et al., 2006; K1250A in Vergani et al., 2003). Since the signature sequence itself is not an ATP binding site before the two NBDs dimerize (Locher et al., 2002; Smith et al., 2002; Lewis et al., 2004), it seems unlikely that the G551D mutation will affect ATP dose–response relationship, which reflects ATP affinity of the closed state when the NBDs are in monomeric configurations. G551D-CFTR activity was examined at different [ATP]. Fig. 8 A shows that the channel activity of G551D-CFTR is not altered even in the presence of 10 mM ATP. These results were further quantified by measuring the ratio of the mean current amplitudes in the presence and absence of ATP. This ratio is ~1 for all [ATP] tested (Fig. 8 B).

We next examined the ATP dependence of G1349D-CFTR more thoroughly by measuring the activity of the channel at different [ATP]. In excised patches, G1349D-CFTR channels were exposed to 2.75 mM ATP + PKA, and then to various ATP concentrations (from 2 μM to 10 mM). The experiments were performed by quantifying G1349D-CFTR channel current at a test [ATP] that was bracketed with 2.75 mM ATP to ensure the absence of a time-dependent rundown (for details see Zeltwanger et al., 1999). Fig. 9 (A and B) shows representative traces for WT- and G1349D-CFTR. Interestingly, the magnitude of current elicited by 50 μM ATP, relative to that with 2.75 mM ATP, is larger for G1349D-CFTR (Fig. 9 B) than for WT-CFTR (Fig. 9 A), suggesting that G1349D-CFTR channels are "more sensitive" to ATP than WT-CFTR. Fig. 9 C shows the normalized ATP dose response for G1349D-CFTR with an overlaid WT-CFTR data for comparison (from Zhou et al., 2006). Interestingly, similar to that of WT- CFTR, the G1349D-CFTR channel activity is saturated at millimolar [ATP], but the ATP dose–response relationship is shifted to the left. Although this mutant has a maximal Po ~10 times lower than WT-CFTR (Fig. 9 D), the open time of the channel is not sensitive to changes in [ATP] (441 ± 30 ms in the presence of 10 μM ATP and 422 ± 33 ms in the presence of 1 mM ATP). These open time constants are not significantly different from the mean open time of WT channels either. Therefore, the difference in the dose response between WT- and G1349D-CFTR (apparent Kd and maximal Po) reflects effects of the mutation on the opening rate of the channel. More interestingly, the dose–response curve of G1349D-CFTR is not as steep as that of WT-CFTR. At low micromolar [ATP], the relative fraction of G1349D current is higher than that of WT. Qualitatively speaking, as the [ATP] is increased, the activity of the G1349D mutant does not increase as much as that of WT channels, as if the increasing activation of G1349D-CFTR upon
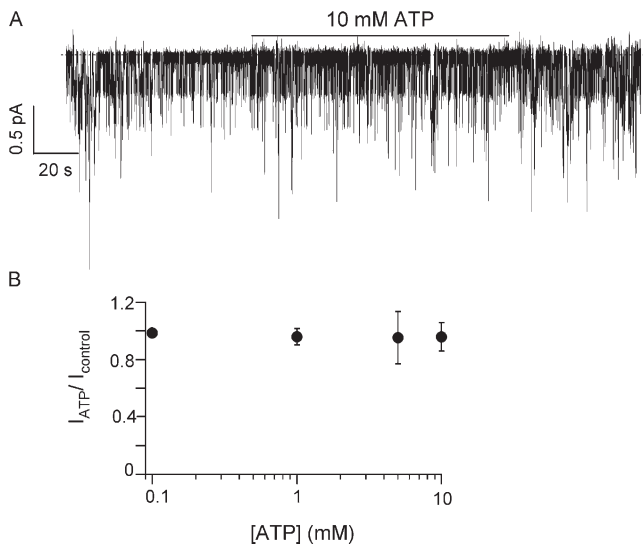
Figure 8. ATP dose–response relationship for G551D-CFTR. (A) Representative trace for G551D-CFTR in the presence of 10 mM ATP. Currents were activated with 1 mM ATP + 25 U/ml PKA (not depicted). (B) Normalized ATP dose–response relationship for G551D-CFTR. Currents at different [ATP] were normalized to the current level in the absence of ATP (washout) ($n = 4$–6 for each data point).

raising [ATP] is accompanied by an inhibitory effect that is also ATP dependent.

Kinetic Modeling for G1349D-CFTR

To explain the unusual ATP dose–response relationship of G1349D-CFTR, we resort to CFTR gating schemes that incorporate two ATP binding sites. We first tried the expanded version of the CFTR gating model proposed

originally by Vergani et al. (2003) (Scheme A in Fig. 10 A), and calculated the steady-state solution for the open probability. In Scheme A, ATP binds either to ABP1 or to ABP2 before the doubly occupied closed state can sojourn to the open state. Hydrolysis of the ATP molecule bound at ABP2 results in channel closing. It was proposed that ATP binding to ABP2 first does not occur frequently for WT-CFTR because of a higher affinity of ABP1 for ATP ($Kd_1 = 10$ µM and $Kd_2 = 40$ µM, from Vergani et al., 2003). We could simulate our WT data using Scheme A. Among the parameters, $ko_{(2ATP)} = 2.5$ s^{-1} and $k_{c(hydro)} = 3$ s^{-1} were obtained from the closed and open time constants of our data (Zhou et al., 2006). Kd_1 (10 µM) was obtained from Vergani et al. (2003), although it should be noted that this value is somewhat arbitrary. Kd_2 (130 µM) was chosen to best fit our ATP dose–response relationship of WT-CFTR (Fig. 10 B).

We then tried to fit the G1349D data using this scheme. To fit the G1349D data we need to be able to reproduce the shift of the curve, the flattening of the slope, as well as an ~10-fold reduced maximal Po. Since the open time for G1349D-CFTR is not significantly different from that of WT channels, $k_{c(hydro)}$ remains unchanged. The only way to obtain a maximal Po 10 times lower than that of WT was to reduce the opening rate ($k_{o(2ATP)}$) from 2.5 s^{-1} to 0.15 s^{-1}. However, the resulting curve (Fig. 10 C, green line; also see Table I) deviates significantly from the data.

Since the G1349 residue is located in the ABP1, we then tested if manipulating the Kd_1 could generate data with a leftward shift of the dose–response curve. Decreasing Kd_1 by as much as 1,000-fold did not produce a
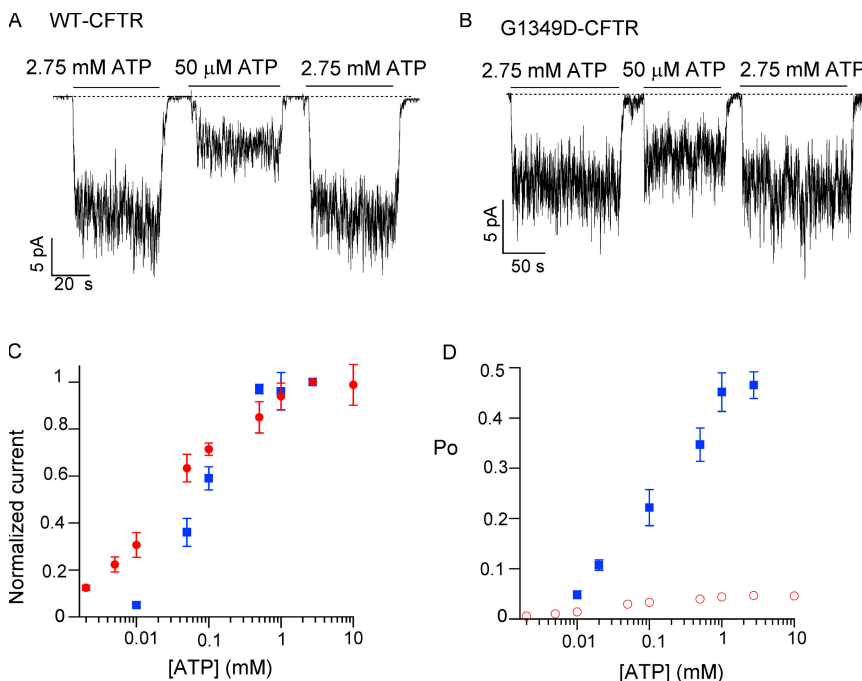

Figure 9. ATP dose–response for G1349D-CFTR. Representative traces of WT- (A) and G1349D-CFTR (B) channels in response to 50 µM and 2.75 mM ATP. Note that the amount of current elicited by 50 µM ATP, relative to the amount of current elicited by 2.75 mM ATP, is larger for G1349D (ratio = 0.65) than for WT (ratio = 0.42) in these particular patches. (C) Normalized ATP dose–response relationship for G1349D-CFTR (red circles) and WT-CFTR (blue squares, from Zhou et al., 2006). (D) Relationships between [ATP] and single-channel Po (blue squares for WT, from Zhou et al., 2006, and red open circles for G1349D). The G1349D Po was calculated under the assumption that the maximal Po is 10 times lower than WT Po.

A Scheme A
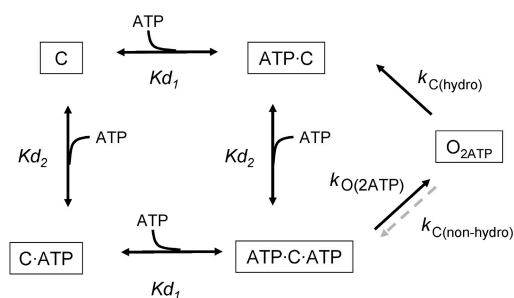
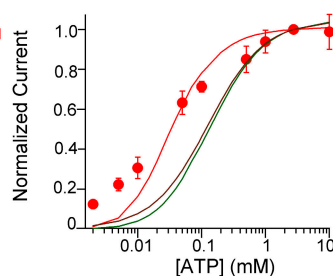**B** WT-CFTR
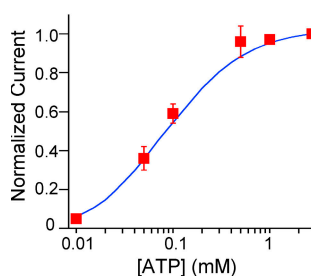
C G1349D-CFTR

Figure 10. (A) Scheme A: a CFTR gating model expanded from one proposed by Vergani et al. (2003). C, ATP·C, and ATP·C·ATP are closed states with no ATP bound, one ATP molecule bound to ABP1, and two ATP molecules bound, respectively. O_{2ATP} is the open state with two bound ATP molecules. Kd_1 and Kd_2 are the dissociation constants of ATP for ABP1 and ABP2, respectively. $k_{O(2ATP)}$ is the opening rate and $k_{C(ATP)}$ is the closing rate of the channel via hydrolysis. The gray arrow, representing the non-hydrolytic closing step, has been ignored in our calculation because it is exceedingly small compared with the closing rate of the hydrolytic closing (same applies to Figure 11). According to this model, the channel can open only after the two binding sites are occupied by ATP. (B) ATP dose response for WT-CFTR channels (red squares) and the simulated curve (blue line) obtained with Scheme A and the parameters summarized in Table I. (C) Normalized ATP dose response for G1349D-CFTR channels (red circles) and different simulated results obtained with Scheme A. The green line represents a fit with the same parameters as WT except for a reduced opening rate. Modification of Kd_1 up to 1,000-fold (brown line) did not reproduce the leftward shift. The red line represents simulated data when the ATP affinity at ABP2 is increased by fivefold (parameters in Table I).

significant shift of the dose–response curve (brown line). On the other hand, increasing Kd_1 resulted in a curve shifted to the right (unpublished data). The leftward shift could be reproduced by reducing Kd_2 by ~5-fold (red line, also see Table I). This fivefold increase in the affinity for ATP at ABP2 seems hard to envision when one considers that G1349 is located at ABP1. The main problem with these results, however, is that they fail to reproduce the flattening of the dose–response curve.

We further expanded Scheme A to include the spontaneous ATP-independent openings that we have observed in various CFTR constructs (Bompadre et al., 2005b; also Fig. 3 above). This addition can be seen

TABLE I
A Summary of the Kinetic Parameters used in Fig. 10 for Scheme A

| Scheme A	WT	A	B	C
Kd_1 (µM)	10	10	0.01	10
Kd_2 (µM)	130	130	130	25
$k_{O(2ATP)}$ (s^{-1})	2.5	0.15	0.15	0.15
$k_{C(hydro)}$ (s^{-1})	3	3	3	3

For WT-CFTR these parameters result in a good fit to the experimental data (Fig. 10 B). The parameter sets A, B, and C correspond to different attempts to fit the G1349D-CFTR data (green, brown, and red lines in Fig. 10 C, respectively).

in Fig. 11 A, Scheme B, enclosed in an orange box. The parameters for the spontaneous openings were obtained from Bompadre et al. (2005b) (measured for ΔR-CFTR), and we assumed that ATP binding to ABP1 has little effect on the ATP-independent opening (i.e., $k_{O(SPT0)} = k_{O(SPT1)} = k_{O(SPT)}$), an assumption supported by Zhou et al. (2006) and the current results with the G551D mutation (see Discussion). We also assumed that the closing rate of both types of spontaneous openings is the same ($k_{c(SPT0)} = k_{c(SPT1)} = k_{c(SPT)}$) since the mean open time of G551D-CFTR is approximately the same as the mean open time of WT channels in the absence of ATP. We calculated the open probability of G1349D-CFTR for this expanded model using the same kinetic parameters listed in Table I with two added new parameters ($k_{c(SPT)} = 2$ s^{-1}; $k_{O(SPT)} = 0.006$ s^{-1}; fromt Bompadre et al., 2005b). Adding this ATP-independent component could not replicate the overall shape of the ATP dose response for G1349D-CFTR (unpublished data).

We then tested the possibility that the G1349D mutation may affect the opening rate for the spontaneous openings. We increased $k_{O(SPT)}$ up to 10-fold, and did not obtain a leftward shift or a less steep curve for the dose–response relationship. The main effect of increasing $k_{O(SPT)}$ is an increase of the relative open probability at low micromolar [ATP], in excess of the measured values. On the other hand, when $k_{c(SPT)}$ and $k_{O(SPT)}$ were kept the same as those of WT channels, the ratio of the G1349D-CFTR current produced by the ATP-independent openings to the maximal current (0.057 ± 0.010) is very close to what the model predicts (0.06). We should point out that even though we could not simulate the flattening of the dose–response relationship for G1349D-CFTR by modifying the opening rate for the spontaneous openings, Kd_2, and the ATP-dependent opening rate ($k_{O(2ATP)}$), we cannot completely rule out the possibility that some combinations of these parameters could produce a curve similar to our data.

Since our previous results implicate a critical role of ATP binding at ABP2, but not at ABP1, in channel opening (Powe et al., 2002; Zhou et al., 2006), we further expanded Scheme A to include the possibility that the

A   Scheme B
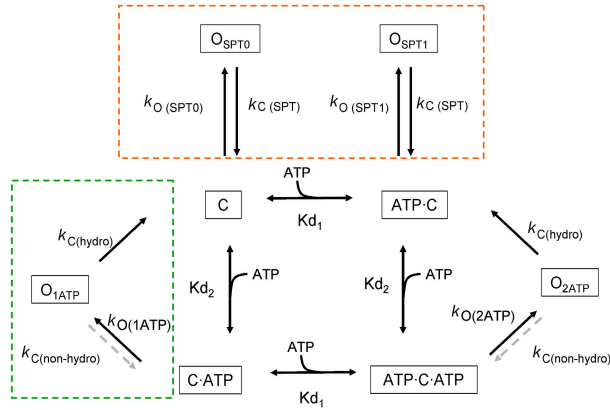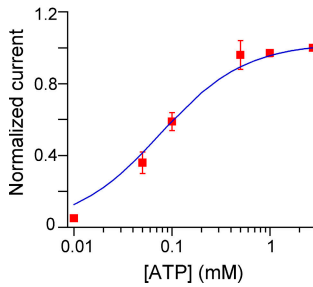
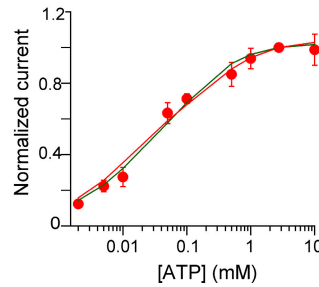

B   WT-CFTR   **C   G1349D-CFTR**

Figure 11. (A) Scheme B: an expanded CFTR gating model proposed in Zhou and Hwang (2007). C, ATP·C, C·ATP, and ATP·C·ATP are closed states with no ATP bound, one ATP bound to ABP1, one ATP bound to ABP2, and both ABP1 and ABP2 occupied, respectively. O_{1ATP} and O_{2ATP} represent open states with only ABP2 occupied by ATP or both ABP1 and ABP2 occupied by ATP, respectively. O_{SPT0} and O_{SPT1} are open states in the ATP-independent component with no ATP or one ATP bound to ABP1, respectively. Kd_1 and Kd_2 are the dissociation constants of ATP for ABP1 and ABP2, respectively. $k_{O\ (1ATP)}$ is the opening rate with ATP bound at ABP2 (from C·ATP to O_{ATP1}); $k_{O\ (2ATP)}$ is the opening rate with ATP binding to ABP1 and ABP2 (from ATP·C·ATP to O_{ATP2}). $k_{C(ATP)}$ is the transition rate from open to closed state in the hydrolytic pathway both without and with ATP binding to ABP1 (from O_{ATP1} to C and from O_{ATP2} to C). $k_{O(SPT)}$ and $k_{C(SPT)}$ are the opening and closing rates for spontaneous ATP-independent gating. (B) Dose–response relationships for WT (red squares) and G1349-CFTR (red circles) and calculated data based on Scheme B and the parameters summarized in Table II

channel may open with just one ATP molecule bound at ABP2 (i.e., ABP1 is vacant). This new addition is depicted with a green box in Fig. 11, Scheme B. This kinetic scheme (Fig. 11, Scheme B) can successfully replicate the WT Po using similar parameters described above, with $k_{O(1ATP)} = k_{O(2ATP)} = 2.5$ s^{-1} (Fig. 11 B, also see summary in Table II). Using Scheme B, we can also obtain a dose–response relationship that reproduces all the features of the G1349D dose response in at least two different ways (Table II). First, without changing any of

TABLE II
A Summary of the Kinetic Parameters used in Fig. 11 for Scheme B

Scheme A	WT	G1349D (a)	G1349D (b)
Kd_1 (µM)	10	10	10
Kd_2 (µM)	130	130	280
$k_{O(1ATP)}$ (s^{-1})	2.5	1	2.5
$k_{O(2ATP)}$ (s^{-1})	2.5	0.16	0.16
$k_{C(hydro)}$ (s^{-1})	3	3	3
$k_{O(SPT)}$ (s^{-1})	0.006	0.006	0.006
$k_{C(SPT)}$ (s^{-1})	2	2	2

These sets of parameters correspond to the fits obtained for WT-CFTR (blue line in Fig. 11 B) and G1349D-CFTR (a corresponds to the green line in Fig. 11 C; b corresponds to the red line in Fig. 11 C).

the WT binding parameters for ABP1 or ABP2, simply reducing $k_{O\ (1ATP)}$ to 1 s^{-1} and $k_{O\ (2ATP)}$ to 0.16 s^{-1} can produce data strikingly similar to those of G1349D-CFTR (green line in Fig. 11 C). The dose–response curve of G1349D-CFTR can also be successfully reproduced by slightly decreasing the affinity for ATP at ABP2 (e.g., by increasing Kd_2 to 280 µM) and simultaneously lowering the opening rate $k_{O\ (2ATP)}$ to 0.16 s^{-1} (red line in Fig. 11 C). These results thus suggest that the G1349D mutation decreases the channel opening rate when ABP1 is occupied by ATP (i.e., $k_{O(2ATP)}$). Possible structural interpretations of this proposition will be discussed below.

DISCUSSION

The data presented in the current studies strongly suggest that the G551D mutation of NBD1 completely eliminates ATP-dependent gating. The residual low activity of G551D-CFTR represents ATP-independent gating events. On the other hand, G1349D-CFTR exhibits a fairly different behavior than G551D-CFTR; it maintains some ATP dependence, but with a lower Po than WT channels due to a lower opening rate. Since G551 and G1349 are located in ABP2 and ABP1, respectively, these results thus support the idea that these two ATP binding sites play different roles in ATP-dependent opening of the channel. We will discuss the fundamental mechanism responsible for the different behavior of these two mutant channels, and the potential clinical implications of our results.

The CFTR protein is composed of five domains: two membrane-spanning domains that form the chloride channel pore; two nucleotide-binding domains (NBD1 and NBD2), defined by the conserved Walker A and B motifs and a signature sequence, that play critical roles in CFTR gating; and a regulatory domain (R domain), phosphorylation of which is essential for channel function. How ATP binding/hydrolysis controls CFTR gating remains controversial despite more than a decade of studies (Gadsby et al., 2006; Zhou and Hwang, 2007).

It is generally agreed that the closure of the channel follows hydrolysis of the ATP molecule by the conserved motifs in NBD2 (i.e., ABP2). For channel opening, one theory predicts that binding of ATP to both ABP1 and ABP2 is required for channel opening (Aleksandrov et al., 2001; Vergani et al., 2003, 2005; Berger et al., 2005). However, Zhou et al. (2006) proposed that binding of ATP to ABP2 catalyzes channel opening, while binding of ATP at ABP1 may not be required (also see Powe et al., 2002; Bompadre et al., 2005b).

The open channel conformation for CFTR likely reflects a head-to-tail NBD dimer (Vergani et al., 2005) seen in other ABC transporters; opening of the channel involves approximation of the two NBDs so that the ATP molecules are sandwiched at the dimer interface. Thus, the individual ABPs are composed of the Walker A and Walker B motifs of one NBD and the signature sequence of the partner NBD (Fig. 1). Previous studies on the role of ATP binding in CFTR gating have been focused mostly on manipulating the Walker A and B motifs (e.g., Powe et al., 2002; Vergani et al., 2003). The current studies on the mutations in the signature sequence provide novel mechanistic insights into how these two ATP binding sites control CFTR gating.

We showed that G551D channels, though still need to be phosphorylated to be functional, do not respond to ATP at all. This lack of response to ATP also explains why the G551D mutant is insensitive to ADP since the main effect of ADP is to competitively inhibit channel opening by ATP (Bompadre et al., 2005a). As mentioned previously, WT-CFTR channels have a finite opening rate in the absence of ATP (Bompadre et al., 2005b; also see Fig. 3 above). If we propose that all the activity observed with the G551D channels represents spontaneous ATP-independent openings, the Po of G551D should be compatible with that of the ATP-independent activity of WT channels. A quick calculation gives a Po of ~0.003 for the ATP-independent activity of WT-CFTR (Po $= \tau_o/(\tau_o + \tau_c)$, where τ_o is the open time of the channel and τ_c is the closed time of the channel from Bompadre et al. (2005b). This value is ~150-fold less than the maximal Po of WT channels. Indeed, in patches containing hundreds of WT channels (e.g., Fig. 3 D), minutes after ATP is removed, ~1% of the macroscopic current still remains. Although it is very difficult, if not impossible, to estimate precisely the Po for G551D from single-channel kinetic analysis, we made a rough estimation by comparing macroscopic current amplitudes between WT and G551D channels if we assume the number of channels in the membrane patches is about the same. Fig. 3 E shows that the average mean current of G551D-CFTR in excised patches is ~120 times smaller than that of WT channels. This result is consistent quantitatively with our hypothesis that G551D-CFTR only exhibits ATP-independent openings.

What is the underlying molecular mechanism responsible for G551D's dysfunction? It should be noted that G551 is located in the signature sequence of NBD1, which, together with the Walker A and B motifs of NBD2, forms ABP2, the site proposed to be critical for channel opening by ATP (Zhou et al., 2006; c.f. Vergani et al., 2003). The G to D mutation either completely abolishes ATP binding at this site, ABP2, or blocks the conformational changes following ATP binding. Biochemical studies of MRP1, an ABC transporter protein belonging to the same subfamily as CFTR, suggest that mutations of this glycine residue in the signature sequence of either NBD have little effect on ATP binding (Ren et al., 2004). Thus, the G551D mutation more likely hampers the conformational changes at ABP2 that facilitate NBD dimerization (i.e., channel opening by ATP). On the other hand, if we assume, here, that the G551D mutation does not affect ATP binding at ABP1 (since the mutation is located at ABP2), the failure of ATP to increase the activity of this mutant supports the notion that ATP binding at ABP1 alone indeed does not catalyze channel opening (Zhou et al., 2006; Scheme B, Fig. 11). Then, G551D-CFTR openings represent spontaneous openings either with no ATP bound at the ABPs or with ATP bound at ABP1. Ultimately, this result reinforces the idea that ATP binding at ABP2 is responsible for the ATP-dependent opening of CFTR. Putting together the current studies and previous work (Powe et al., 2002; Zhou et al., 2006), we have established an asymmetrical role of the two ABPs in CFTR gating. It is worth to note that Cai et al. (2006) reported that 2'-deoxy ATP can potentiate G551D-CFTR channel activity. It will be interesting to investigate how and where this ATP analogue exerts its effects.

In contrast to G551D-CFTR, G1349D-CFTR still maintains some ATP dependence, but has a maximal Po ~10-fold lower than WT-CFTR. It is interesting to note that the inhibition of G1349D-CFTR channels by ADP is slightly smaller than the inhibition of WT channels. To explain this observation we have to realize that G1349D channels also have ATP-independent openings, and because of a much lower Po at maximal [ATP], the fraction of the total current that originates from the ATP-independent openings is relatively higher in G1349D than in WT channels. Since the ATP-independent activity is insensitive to ADP, the portion of the total current that can be inhibited by ADP is relatively smaller in G1349D than WT channels.

If binding of ATP to ABP1 is not essential for channel opening as described above, why does the G1349D mutation, located at ABP1, decrease the maximal Po? Since the open time of the mutant channel does not differ significantly from that of WT channels, we can conclude that the defect of G1349D-CFTR resides in a lowered opening rate. However, this mutation does not appear

to decrease ATP binding affinity because, first, the current saturates at millimolar [ATP], and, second, the ATP dose–response relationship is shifted to the left by the mutation (Fig. 9 C). The most intriguing feature of G1349D-CFTR is the flattened ATP dose–response curve, suggesting a negative cooperativity between the two ATP binding sites. Based on the results of our modeling, we propose that this negative cooperativity seen with the G1349D mutation arises from a negative effect on channel opening by ATP binding at ABP1.

Although our calculations provide, at a minimum, two different solutions, we prefer the one in which both opening rates are diminished ($k_{O\ (1ATP)} = 1\ s^{-1}$ and $k_{O\ (2ATP)} = 0.16\ s^{-1}$) because this kinetic explanation corroborates with recent structural interpretations of CFTR gating (Vergani et al., 2005; Zhou et al., 2006). The opening of CFTR is coupled to the dimerization of CFTR's two NBDs (Vergani et al., 2005). Zhou et al. (2006) further proposed that the opening of the channel (i.e., dimerization of CFTR's two NBDs) is initiated by ATP binding to ABP2 irrespectively of whether ABP1 is occupied or not, but the final approximation of the two parts that form ABP1 precedes channel opening. Compared with glycine, aspartate has a negatively charged side chain. This side chain by itself may sterically hinder NBD dimerization even when ABP1 is not occupied by ATP (i.e., a reduced $k_{O(1ATP)}$). Since the D1349 residue should also be physically close to the bound ATP when the two NBDs are approaching each other upon dimerization (Lu et al., 2005), it is possible that the electrostatic repulsion between the negatively charged ATP and the negative charge of the aspartate at position 1349 hinders the dimerization process even more (i.e., an even smaller $k_{O(2ATP)}$). Future studies using different mutations at this position and/or nearby amino acids should provide further insight into the molecular mechanism of the gating defects manifested in this CF-associated mutant.

It is interesting to note that AMP-PNP does not lock open either G551D or G1349D channels. It is known that AMP-PNP locks open WT channels after they are first opened by ATP (Gunderson and Kopito, 1994; Hwang et al., 1994). Thus AMP-PNP likely binds to a state following the ATP-induced open channel conformation. In the case of G551D, it is not surprising that we do not see any effects with AMP-PNP because this mutation completely eliminates ATP-dependent gating. It is however puzzling that AMP-PNP is ineffective on G1349D-CFTR. Interestingly, Cai et al. (2006) reported that pyrophosphate, an agent that potentiates CFTR by a similar mechanism as AMP-PNP, also fails to act on G1349D-CFTR. Perhaps, the aspartate side chain of G1349D-CFTR prevents the formation of a stable locked-open conformation. A similar mechanism may also account for the lack of effect on the open time of G1349D-CFTR by removing free Mg^{2+}.

In addition to the mechanistic insights into how CFTR's two NBDs work concertedly to gate the channel, our observations also provide a quantitative explanation for the different phenotypes exhibited in CF patients carrying the G551D or G1349D mutation. Since these two mutations affect neither membrane trafficking nor the single-channel amplitude, the reduction of the maximal current by these mutations results solely from a decrease in Po. Although it is unknown exactly how much functional defect of CFTR is needed to cause CF, our data suggest that a 10-fold decrease of maximal CFTR channel activity results in mild form CF (compare Sheppard et al., 1993). On the other hand, a 100-fold decrease of maximal CFTR channel activity is sufficient to cause severe form CF (compare Wang et al., 2000). This quantitative relationship between CFTR activity and clinical phenotypes is similar to that proposed previously by Davis (2001). Future studies of other disease-associated mutations can lead to a more quantitative understanding of the pathophysiology of CF, which will then serve to guide therapeutic development for patients with CF.

Many CFTR potentiators have been shown to increase the currents of one or both of these mutants, sometimes with different potencies (Becq et al., 1994; Becq et al., 1996; Illek et al., 1999; Ai et al., 2004; Moran et al., 2005; Pedemonte et al., 2005; Cai et al., 2006). The mechanism by which these CFTR activators work remains unclear (Hwang and Sheppard, 1999; Hwang et al., 2003). Since genistein increases the activity of G551D-CFTR (e.g., Illek et al., 1999) our results suggest that genistein's action may involve more than a simple effect on ATP-dependent gating as previously proposed (Weinreich, et al., 1997; Wang et al., 1998). Nevertheless, it is interesting to note that 20 μM genistein increases G1349D-CFTR current density 6.8 ± 1.9-fold ($n = 14$) compared with forskolin alone. With this increase, G1349D current density is $\sim$60% of that of WT, a level likely sufficient to completely restore the physiological function of chloride secretion. On the other hand, 20 μM genistein increases G551D current density by 6.5 ± 2.4-fold ($n = 19$). This may be adequate to reach a level of activity similar to that of G1349D-CFTR but unlikely to completely restore the physiological function of this mutant channel. Thus, we believe that the current results provide considerable mechanistic information for future pharmacological studies, which in turn could pave the way for a tailored drug design for therapeutical interventions in CF.

REFERENCES

Ai, T., S.G. Bompadre, X. Wang, S. Hu, M. Li, and T.-C. Hwang. 2004. Capsaicin potentiates wild-type and mutant CFTR chloride channel currents. *Mol. Pharmacol.* 65:1415–1426.

Aleksandrov, L., A. Mengos, X.-B. Chang, A. Aleksandrov, and J.R. Riordan. 2001. Differential interactions of nucleotides at the two nucleotide binding domains of the cystic fibrosis transmembrane conductance regulator. *J. Biol. Chem.* 276:12918–12923.

Anderson, M.P., and M.J. Welsh. 1992. Regulation by ATP and ADP of CFTR chloride channels that contain mutant nucleotide-binding domains. *Science.* 257:1701–1704.

Beaudet, A.L., G.L. Feldman, K. Kobayashi, W.K. Lemma, S.D. Fernbach, M.R. Knowles, R.C. Boucher, and W.E. O'Brien. 1991. Mutation analysis for cystic fibrosis in a North American population. *In* The Identification of the CF (cystic fibrosis) Gene-recent Progress and New Research Strategies. L-C. Tsui, G. Romeo, R. Greger, and S. Gorini, editors. Plenum Press, New York. 53–54.

Becq, F., T.J. Jensen, X.B. Chang, A. Savoia, J.M. Rommens, L.C. Tsui, M. Buchwald, J.R. Riordan, and J.W. Hanrahan. 1994. Phosphatase inhibitors activate normal and defective CFTR chloride channels. *Proc. Natl. Acad. Sci. USA.* 91:9160–9164.

Becq, F., B. Verrier, X.B. Chang, J.R. Riordan, and J.W. Hanrahan. 1996. cAMP- and Ca^{2+}-independent activation of cystic fibrosis transmembrane conductance regulator channels by phenylimidazothiazole drugs. *J. Biol. Chem.* 271:16171–16179.

Berger, A.L., M. Ikuma, and M.J. Welsh. 2005. Normal gating of CFTR requires ATP binding to both nucleotide-binding domains and hydrolysis at the second nucleotide-binding domain. *Proc. Natl. Acad. Sci. USA.* 102:455–460.

Bompadre, S.G., T. Ai, J.H. Cho, X. Wang, Y. Sohma, M. Li, and T.-C. Hwang. 2005a. CFTR gating I: characterization of the ATP-dependent gating of a phosphorylation-independent CFTR construct (ΔR-CFTR). *J. Gen. Physiol.* 125:361–375.

Bompadre, S.G., J.H. Cho, X. Wang, X. Zou, Y. Sohma, M. Li, and T.-C. Hwang. 2005b. CFTR gating II: effects of nucleotide binding on the stability of open states. *J. Gen. Physiol.* 125:377–394.

Brancolini, V., L. Cremonesi, E. Belloni, E. Pappalardo, R. Bordoni, M. Seia, S. Russo, R. Padoan, A. Giunta, and M. Ferrari. 1995. Search for mutations in pancreatic sufficient cystic fibrosis Italian patients: detection of 90% of molecular defects and identification of three novel mutations. *Hum. Genet.* 96:312–318.

Cai, Z., A. Taddei, and D.N. Sheppard. 2006. Differential sensitivity of the cystic fibrosis (CF)-associated mutants G551D and G1349D to potentiators of the cystic fibrosis transmembrane conductance regulator (CFTR) Cl⁻ channel. *J. Biol. Chem.* 281:1970–1977.

Chang, X.-B., J.A. Tabcharani, Y.-X. Hou, T.J. Jensen, N. Kartner, N.W. Alon, J.W. Hanrahan, and J.R. Riordan. 1993. Protein kinase A (PKA) still activates CFTR chloride channel after mutagenesis of all 10 PKA consensus phosphorylation sites. *J. Biol. Chem.* 268:11304–11311.

Colquhoun, D., and A.G. Hawkes. 1995. A Q-matrix cookbook: how to write only one program to calculate the single-channel and macroscopic prediction for any kinetic mechanism. *In* Single-Channel Recording. B. Sakmann, and E. Neher, editors. Plenum Press, New York. 589–633.

Csanády, L. 2000. Rapid kinetic analysis of multichannel records by a simultaneous fit to all dwell-time histograms. *Biophys. J.* 78:785–799.

Cutting, G.R., L.M. Kasch, B.J. Rosenstein, J. Zielenski, L.C. Tsui, S.E. Antonarakis, and H.H. Kazazian Jr. 1990. A cluster of cystic fibrosis mutations in the first nucleotide-binding fold of the cystic fibrosis conductance regulator protein. *Nature.* 346:366–369.

Davis, P.B. 2001. Cystic Fibrosis. *Pediatr. Rev.* 22:257–264.

Dousmanis, A.G., A.C. Nairn, and D.C. Gadsby. 2002. Distinct Mg^{2+}-dependent steps rate limit opening and closing of a single CFTR Cl channel. *J. Gen. Physiol.* 119:545–559.

Drumm, M.L., D.J. Wilkinson, L.S. Smit, R.T. Worrell, T.V. Strong, R.A. Frizzell, D.C. Dawson, and F.S. Collins. 1991. Choride conductance expressed by ΔF508 and other mutant CFTRs in *Xenopus* oocytes. *Science.* 254:1797–1799.

Gadsby, D.C., P. Vergani, and L. Csanady. 2006. The ABC protein turned chloride channel whose failure causes cystic fibrosis. *Nature.* 440:477–483.

Galietta, L.J., M.F. Springsteel, M. Eda, E.J. Niedzinski, K. By, M.J. Haddadin, M.J. Kurth, M.H. Nantz, and A.S. Verkman. 2001. Novel CFTR chloride channel activators identified by screening of combinatorial libraries based on flavone and benzoquinolizinium lead compounds. *J. Biol. Chem.* 276:19723–19728.

Gregory, R.J., D.P. Rich, S.H. Cheng, D.W. Souza, S. Paul, P. Manavalan, M.P. Anderson, M.J. Welsh, and A.E. Smith. 1991. Maturation and function of the cystic fibrosis transmembrane regulator variants bearing mutations in putative nucleotide-binding domains 1 and 2. *Mol. Cell. Biol.* 11:3886–3893.

Gunderson, K.L., and R.R. Kopito. 1994. Effects of pyrophosphate and nucleotide analogs suggest a role for ATP hydrolysis in cystic fibrosis transmembrane regulator channel gating. *J. Biol. Chem.* 269:19349–19353.

Hwang, T.-C., and D.N. Sheppard. 1999. Molecular pharmacology of the CFTR Cl⁻ channel. *Trends Pharmacol. Sci.* 20:448–453.

Hwang, T.-C., G. Nagel, A.C. Nairn, and D.C. Gadsby. 1994. Regulation of the gating of cystic fibrosis transmembrane conductance regulator C1 channels by phosphorylation and ATP hydrolysis. *Proc. Natl. Acad. Sci. USA.* 91:4698–4702.

Hwang, T.-C., R.E. Koeppe, and O.S. Andersen. 2003. Genistein can modulate channel function by a phosphorylation-independent mechanism: importance of hydrophobic mismatch and bilayer mechanics. *Biochemistry.* 42:13646–13658.

Illek, B., L. Zhang, N.C. Lewis, R.B. Moss, J.Y. Dong, and H. Fischer. 1999. Defective function of the cystic fibrosis-causing missense mutation G551D is recovered by genistein. *Am. J. Physiol.* 277:C833–C839.

Kerem, B.-S., J. Zielenski, D. Markiewicz, D. Bozon, E. Gazit, J. Yahav, D. Kennedy, J.R. Riordan, F.S. Collins, J.M. Rommens, and L.-C. Tsui. 1990. Identification of mutations in regions corresponding to the two putative nucleotide (ATP)-binding folds of the cystic fibrosis gene. *Proc. Natl. Acad. Sci. USA.* 87:8447–8451.

Lewis, H.A., S.G. Buchanan, S.K. Burley, K. Conners, M. Dickey, M. Dorwart, R. Fowler, X. Gao, W.B. Gruggino, W.A. Hendrickson, et al. 2004. Structure of nucleotide-binding domain 1 of the cystic fibrosis transmembrane conductance regulator. *EMBO J.* 23:282–293.

Li, C., M. Ramjeesingh, W. Wang, E. Garami, M. Hewryk, D. Lee, J.M. Rommens, K. Galley, and C.E. Bear. 1996. ATPase activity of the cystic fibrosis transmembrane conductance regulator. *J. Biol. Chem.* 271:28463–28468.

Locher, K.P., A.T. Lee, and D.C. Rees. 2002. The *E. coli* BtuCD structure: a framework for ABC transporter architecture and mechanism. *Science.* 296:1091–1098.

Logan, J., D. Hiestand, P. Daram, Z. Huang, D.D. Muccio, J. Hartman, B. Haley, W.J. Cook, and E.J. Sorscher. 1994. Cystic fibrosis transmembrane conductance regulator mutations that disrupt nucleotide binding. *J. Clin. Invest.* 94:228–236.

Lu, G., J.M. Westbrooks, A.L. Davidson, and J. Chen. 2005. ATP hydrolysis is required to reset the ATP-binding cassette dimer into the resting-state conformation. *Proc. Natl. Acad. Sci. USA.* 102:17969–17974.

Mathews, C.J., J.A. Tabcharani, and J.W. Hanrahan. 1998. The CFTR chloride channel nucleotide interactions and temperature-dependent gating. *J. Membr. Biol.* 163:55–66.

Moran, O., L.J. Galietta, and O. Zegarra-Moran. 2005. Binding site of activators of the cystic fibrosis transmembrane conductance regulator in the nucleotide binding domains. *Cell. Mol. Life Sci.* 62:446–460.

Pedemonte, N., N.D. Sonawane, A. Taddei, J. Hu, O. Zegarra-Moran, Y.F. Suen, L.I. Robins, C.W. Dicus, D. Willenbring, M.H. Nantz, et al. 2005. Phenylglycine and sulfonamide correctors of defective ΔF508 and G551D cystic fibrosis transmembrane conductance regulator chloride-channel gating. *Mol. Pharmacol.* 67:1797–1807.

Powe, A., L. Al-Nakkash, M. Li, and T.-C. Hwang. 2002. Mutation of Walker-A lysine 464 in cystic fibrosis transmembrane conductance regulator reveals functional interaction between its nucleotide binding domains. *J. Physiol.* 539:333–346.

Quinton, P.M. 1990. Cystic fibrosis: a disease in electrolyte transport. *FASEB J.* 4:2709–2717.

Ren, X.Q., T. Furukawa, M. Haraguchi, T. Sumizawa, S. Aoki, M. Kobayashi, and S. Akiyama. 2004. Function of the ABC signature sequences in human multidrug resistance protein 1. *Mol. Pharmacol.* 65:1536–1542.

Riordan, J.R., J.M. Rommens, B.-S. Kerem, N. Alon, R. Rozmahel, Z. Grzelzak, J. Zielenski, S. Lok, N. Plavsic, J.-L. Chou, et al. 1989. Identification of the cystic fibrosis gene: cloning and characterization of complementary DNA. *Science.* 245:1066–1072.

Salvatore, F., O. Scudiero, and G. Castaldo. 2002. Genotype-phenotype correlations in cystic fibrosis: the role of modifier genes. *Am. J. Med. Genet.* 111:88–95.

Sheppard, D.N., D.P. Rich, L.S. Ostedgaard, R.J. Gregory, A.E. Smith, and M.J. Welsh. 1993. Mutations in CFTR associated with mild-disease-form Cl⁻ channels with altered pore properties. *Nature.* 362:160–164.

Smith, P.C., N. Karpowich, L. Millen, J.E. Moody, J. Rosen, P.J. Thomas, and J.F. Hunt. 2002. ATP binding to the motor domain from an ABC transporter drives formation of a nucleotide sandwich dimer. *Mol. Cell.* 10:139–149.

Tsui, L.-C., and P. Durie. 1997. Genotype and phenotype in cystic fibrosis. *Hosp. Pract.* 32:115–118, 123–129, 134.

Vergani, P., A.C. Nairn, and D.C. Gadsby. 2003. On the mechanism of MgATP-dependent gating of CFTR Cl⁻ channels. *J. Gen. Physiol.* 121(1):17–36.

Vergani, P., S.W. Lockless, A.C. Nairn, and D.C. Gadsby. 2005. CFTR opening by ATP-driven tight dimerization of its nucleotide binding domains. *Nature.* 433:876–880.

Wang, F., S. Zeltwanger, I. Yang, A. Nairn, and T.-C. Hwang. 1998. Action of genistein on CFTR gating: evidence of two binding sites with opposite effects. *J. Gen. Physiol.* 111:477–490.

Wang, F., S. Zeltwanger, S. Hu, and T.-C. Hwang. 2000. Deletion of phenylalanine 508 causes attenuated phosphorylation-dependent activation of CFTR chloride channels. *J. Physiol.* 524:637–648.

Wang, W., K. Bernard, G. Li, and K.L. Kirk. 2007. Curcumin opens CFTR channels by a novel mechanism that requires neither ATP binding NOR dimerization of the nucleotide binding domains. *J. Biol. Chem.* 282:4533–4544.

Weinreich, F., P.G. Wood, J.R. Riordan, and G. Nagel. 1997. Direct action of genistein on CFTR. *Pflugers Arch.* 434:484–491.

Welsh, M.J., and A.E. Smith. 1993. Molecular mechanisms of the CFTR chloride channel dysfunction in cystic fibrosis. *Cell.* 73:1251–1254.

Wilkinson, D.J., M.K. Mansoura, P.Y. Watson, L.S. Smit, F.S. Collins, and D.C. Dawson. 1996. CFTR: the nucleotide binding folds regulate the accessibility and stability of the activated state. *J. Gen. Physiol.* 107:103–119.

Winter, M.C., D.N. Sheppard, M.R. Carson, and M.J. Welsh. 1994. Effect of ATP concentration on CFTR Cl⁻ channels: a kinetic analysis of channel regulation. *Biophys. J.* 66:1398–1403.

Zeltwanger, S., F. Wang, G.T. Wang, K.D. Gillis, and T.-C. Hwang. 1999. Gating of cystic fibrosis transmembrane conductance regulator chloride channels by adenosine triphosphate hydrolysis. Quantitative analysis of a cyclic gating scheme. *J. Gen. Physiol.* 113:541–554.

Zhou, Z., S. Hu, and T.-C. Hwang. 2001. Voltage-dependent flickery block of an open cystic fibrosis transmembrane conductance regulator (CFTR) channel pore. *J. Physiol.* 532:435–448.

Zhou, Z., S. Hu, and T.-C. Hwang. 2002. Probing an open CFTR pore with organic anion blockers. *J. Physiol.* 120:647–662.

Zhou, Z., X. Wang, M. Li, Y. Sohma, X. Zou, and T.-C. Hwang. 2005. High affinity ATP/ADP analogs as new tools for studying CFTR gating. *J. Physiol.* 569:447–457.

Zhou, Z., X. Wang, H.-Y. Liu, X. Zou, M. Li, and T.-C. Hwang. 2006. The two ATP binding sites of the cystic fibrosis transmembrane conductance regulator (CFTR) play distinct roles in gating kinetics and energetics. *J. Gen. Physiol.* 128:413–422.

Zhou, Z., and T.-C. Hwang. 2007. Gating of the cystic fibrosis transmembrane regulator (CFTR) chloride channels. *In* Advances in Molecular Biology, 38. E.E. Bittar, editor. Elsevier, New York. 145–180.